

Proceedings of Meetings on Acoustics

Volume 17, 2012

<http://acousticalsociety.org/>

ECUA 2012 11th European Conference on Underwater Acoustics
Edinburgh, Scotland
2 - 6 July 2012
Session UW: Underwater Acoustics

UW74. Acoustic prediction using a feature-oriented regional modeling system and acoustic inversion

Gabriel Codato*, Leandro Calado, Néelson E. Martins, Wandrey D. Watanabe, Ricardo M. Domingues and S. M. Jesus

***Corresponding author's address: Departamento de Pesquisas, IEAPM, Brazilian Navy, Rua Kioto, 253 - Praia dos Anjos, Arraial do Cabo, 28930000, Rio de Janeiro, Brazil, gabrielcodato@gmail.com**

Acoustic prediction for future time frames usually suffer from uncertainties in ocean forecasts, due to the extreme sensitivity of acoustic propagation to the ocean environment. The current work assesses the feasibility of combining a Feature-Oriented Regional Modeling System (FORMS) with acoustic inversion outcomes, for acoustic prediction in the Cabo Frio (Brazil) coastal area. First, the oceanographic prediction model is tested for acoustic applications. Two numerical acoustic simulations were performed, with an acoustic model having as input two different initial fields: i) in situ hydrographic data from the OAE_{x10} sea trial, and ii) the oceanographic modeling system outputs. The simulations were compared in terms of transmission loss (TL), detection probability and impulse response. The second stage of this work concerned acoustic data-model comparison, for OAE_{x10}. Experimental impulse responses correlated fairly well with modeled ones corresponding to the forecasts, with values between 0.72 and 0.89. In an attempt to increase these values, the acoustic data was inverted, for the basement compressional speed, whose estimates led to increased impulse response correlations of as high as 0.96. In summary, the prediction of the acoustic field can be well accomplished by combining a FORMS technique with an acoustic inversion scheme.

Published by the Acoustical Society of America through the American Institute of Physics

1 INTRODUCTION AND BACKGROUND

Acoustic propagation is extremely sensitive to the physical oceanographic environment, through the sound speed field. The latter is a function of density in sea water, which forces the temperature and salinity distribution, stratification and dynamics, to play a key role on the propagation of acoustic energy. Furthermore, multiple interactions of sound waves with the seabed lead to peculiar propagation effects, especially in shallow waters [1]. A significant research effort has been triggered in this respect, recognizing ocean-acoustics as an interdisciplinary science. In particular, there is a special interest in understanding the impact of environmental variability on acoustic predictions and sonar performance. This question has been addressed in past work [2–5]. Acoustic prediction uncertainties have been quantified, with the results explained through dynamical sensitivities [6, 7]. In summary, the above studies emphasized that the error on acoustic prediction is highly dependent on the ocean forecast error and on the accuracy of bathymetric/geoacoustic properties. For this reason, methods and systems built to forecast the acoustic field, must be sustained by increasingly sophisticated oceanographic modeling systems, and reliable sea bottom data.

This work aims at evaluating the feasibility of combining a Feature-Oriented Regional Modeling System (FORMS) with acoustic inversion outcomes, for acoustic prediction in the Cabo Frio – Brazil (23°S) coastal area. FORMS consists of a technique based on the construction of realistic oceanic structures, using a ‘feature model’ approach [8]. Feature models are simple mathematical representations of ocean features (e.g. currents, fronts, eddies), which are parameterized in terms of their synoptic characteristics: temperature (T), salinity (S), and velocity components (u, v). The rationale of this approach is to develop a first-order system in a much more complex nonlinear system such as a regional ocean, where most processes strongly interact and cannot be studied separately. Once the first-order structures are placed within a numerical model dynamical framework, the nonlinearity stimulates further interaction among features and creates realistic four-dimensional complex fields [9]. In this regard, the feature modeling technique is widely used to supply nowcasting and forecasting systems with realistic ocean data [10–12].

In the past, feature models were also pointed out as a feasible means of interfacing ocean dynamical models with underwater-acoustic propagation models [13]. It was shown that feature models can reproduce the main acoustic properties of the ocean environment [14]. In the current study, an ocean forecasting model was initialized by a parametric feature model for the Cabo Frio coastal upwelling system. The guidelines of the present approach aim at representing the dynamics of the Cabo Frio coastal region in a realistic fashion. In that region, the upwelling is of utmost importance, both in oceanographic and acoustic terms, due to the induction of strong horizontal temperature gradients. The latter cause a strong impact on the acoustic pressure field, as shown in previous works [15, 16]. In the present work, the effect of upwelling on the prediction of transmission loss (TL), detection probability (DP) and the acoustic channel impulse response is investigated.

Taking into account that the prediction of the acoustic field relies heavily on a given acoustic propagation model, parametrized by several environmental parameters, the determination of appropriate

values for those parameters is of paramount importance. The information regarding these parameters can be provided by ocean sampling procedures, which are limited by a space-time dependent ocean. This limitation can be overcome in situations in which it is possible to probe the ocean with acoustic signals, which, by acoustic inversion procedures, allow to estimate the environmental parameters influencing the observed acoustic propagation characteristics. At last, and as shown in the present work, the values estimated by acoustic inversion are optimal in the sense of modeling the acoustic field. This implies that an inversion procedure is a valuable tool in an acoustic prediction exercise, which can compensate for possible propagation modeling inaccuracies. In the past, it was already observed, through data/model comparisons, that acoustic inversion methods can play an important role in minimizing the variance of sonar performance prediction [17, 18]. In the current study, the acoustic data were inverted for the basement compressional speed, in an attempt to 'fine tune' the geoacoustic parameters on the subjacent acoustic prediction system.

This work is presented in two stages. In the first stage, the present work quantifies the ability of the feature-oriented ocean forecast system for acoustical applications. Two numerical acoustic simulations were performed, with a propagation model having as input: (i) the *in situ* oceanographic data from the Ocean Acoustic Exploration 2010 (OAE10) sea trial, and (ii) the oceanographic modeling system output. In the second stage, the acoustic predictions are compared with acoustic data acquired on the OAE10 experiment, in order to quantify the forecast uncertainty. In predicting the acoustic field, an acoustic inversion technique is used to provide accurate ocean bottom information.

This article is organized as follows: Section 2 describes the OAE10 experiment and the oceanographic-acoustical prediction system; Section 3 presents numerical simulation results and data/model comparisons; Section 4 concludes the paper.

2 COUPLED OCEANOGRAPHIC-ACOUSTICAL PREDICTION SYSTEM

2.1 THE OAE10 EXPERIMENT

The OAE10 sea trial took place along the coast of Cabo Frio (southeastern Brazil), during the period of November 19–21, 2010. It was a multi-institutional and multi-disciplinary exercise, involving oceanographical and acoustical surveys aboard of two Brazilian Navy's vessels (R/V *Aspirante Moura* and EDCG *Guarapari*). The region around Cabo Frio provides a unique environment, where the coast orientation changes and continental shelf break topography reinforces the interaction between the oceanic and coastal systems [19]. This region can have different wind and wave regimes, depending upon the presence of meteorological frontal systems and of mesoscale oceanographic features (e.g. upwelling, eddies, meanders, etc.).

The sea trial was designed to obtain a synoptic horizontal grid covering the coastal upwelling feature around Cabo Frio. A complete CTD (conductivity, temperature and depth) sampling was performed throughout the experiment, yielding vertical profiles of temperature and salinity (Fig. 1). The combination of such profiles on a T-S diagram (see Fig. 1 – right panel) allowed to confirm the occurrence of an upwelling phenomenon. It was found that the thermohaline index from CTD casts corresponded to the South Atlantic Central Water (SACW) water mass index, as proposed in [20]. The SACW is a water mass characterized by temperatures lower than 18 °C, which rises at the surface in the vicinity of Cabo Frio, and represents an upwelling indicator [11]. In particular, a temporal evolution of an upwelling process was observed for three days, during the trial period. This was recorded by the displacement of the upwelling front toward the ocean and the cooling of surface waters at stations closer to the coast, which can be observed on the interpolated sea surface temperature (SST) maps generated from CTD data, shown in Fig. 2. Processed CTD data were interpolated using an Objective Analysis (OA) scheme, with horizontal resolution of 1 km and 30 vertical levels. For the first stage of this paper, the objectively analyzed T-S fields allowed to derive sound-speed sections, to use as environmental parameters for acoustic model initialization. From now on, this dataset is referred to as the OAE10 ocean data.

The acoustic propagation experiments were conducted with a sound source emitting sequences of continuous waves (CW) signals and linearly frequency modulated (LFM) signals. Focus is to the data acquired on November 19, 2010, during the active acoustic measurements at the upwelling front site. The R/V *Aspirante Moura* was the transmitting ship, and deployed the sound source at 10 m depth. The EDCG *Guarapari* deployed a vertical receiving array with 8 hydrophones 3-m spaced, from 10-m to 31-m depth. The distance between source and hydrophone array was 1395 m. The OAEx10 acoustic-data is composed by a sequence of ten LFM signals from 500Hz to 1kHz (low band), a sequence of LFM signals from 1 to 2kHz (high band) and a CW multi-tone from 500Hz to 2kHz with nine intermediate frequencies.

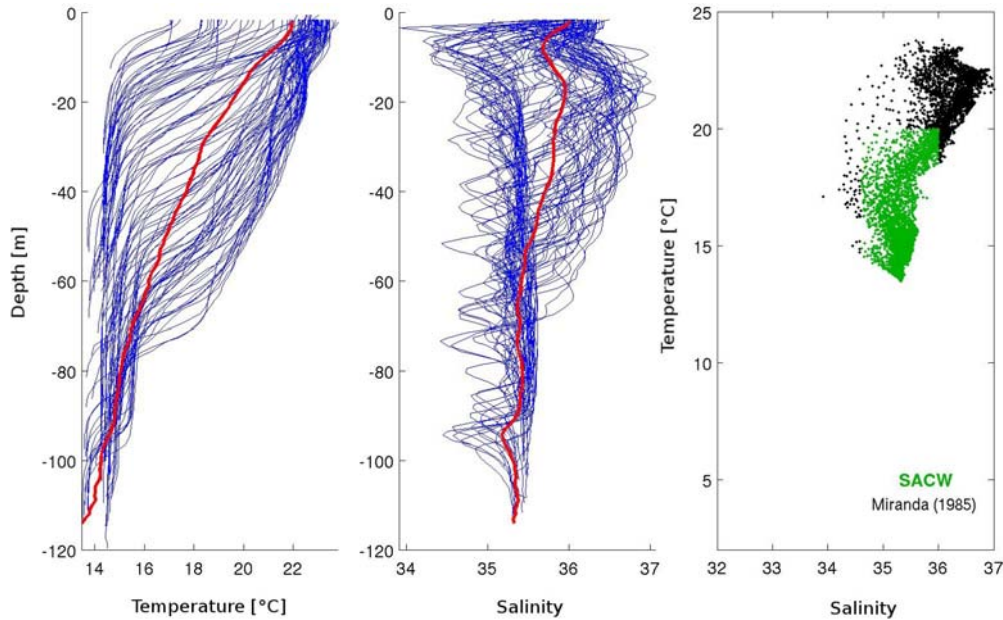


Figure 1: CTD profiles collected during OAEx10 sea trial. (Left) Temperature vs. depth. (Center) Salinity vs. depth. (Right) T-S diagram, where the green points correspond to the SACW water mass, which is an upwelling indicator.

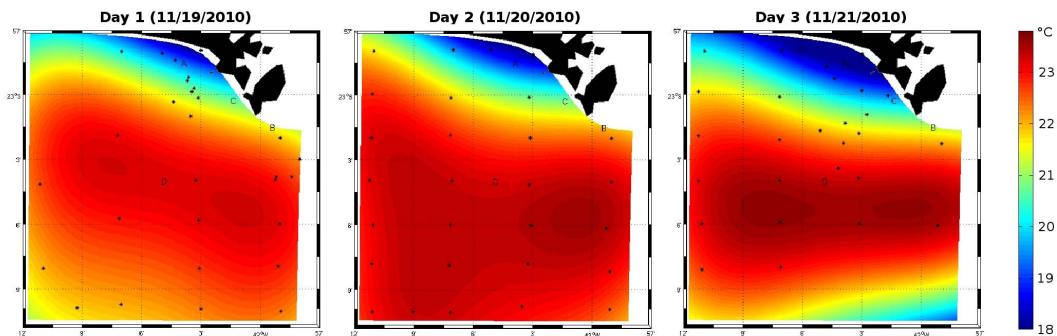


Figure 2: SST snapshots based on the interpolated OAEx10 ocean-data, showing the coastal upwelling registered on November 19th, 20th and 21th, respectively. The black dots represent the CTD sampling stations.

2.2 OCEANOGRAPHIC MODELING SYSTEM

The oceanographic modeling system was based on the methodology presented in [9], which was derived from the FORMS initialization technique developed in ref. [8], which generalizes the feature modeling approach for strategic application to any oceanic region. The generalization can be summarized as a three-step procedure: i) a regional synoptic feature-oriented circulation template is developed via a synthesis of past observational studies in the region; ii) individual feature models for each of the features are developed from synoptic observational studies; iii) the feature model profiles on the template locations are interpolated with appropriate background climatology to obtain a three-dimensional synoptic grid ready for the numerical model applications. The present work applied a variation of this technique for the coastal upwelling associated with the SACW water mass in the vicinity of Cabo Frio coast. The employed FORMS methodology is described below.

2.2.1 The Feature-Oriented Regional Model

The feature-oriented regional model consists on the combination of a coastal upwelling parametric feature model with a background climatological thermohaline structure from the World Ocean Atlas – WOA'05 [21]. The synoptic water mass (*T-S*) structures used for the upwelling parametrization were characterized from the 'Dinâmica do Ecosistema da Plataforma da Região Oeste do Atlântico Sul – DEPROAS' dataset, which was described in more detail in previous work [9].

A schematic representation of the proposed feature model is shown in Fig. 3. It is derived from the continental shelf-slope front feature model developed by [8], and updated by [9] and [22]. The upwelling frontal temperature distribution $T(\eta, z)$ is parameterized as:

$$T(\eta, z) = T_o(z) + [T_i(z) - T_o(z)]m(\eta, z), \quad (1)$$

where

$$m(\eta, z) = 0.5 + 0.5 \tanh \left[\frac{\eta - \Theta z}{\chi} \right] \quad (2)$$

is a meld function, η is the cross-frontal distance from the axis of the front, and z is positive vertically upward. $T_i(z)$ is the inshore temperature profile, and $T_o(z)$ is the offshore temperature profile. Θ is the slope of the front, and χ is the e-folding half-width of the front ($= r/2$).

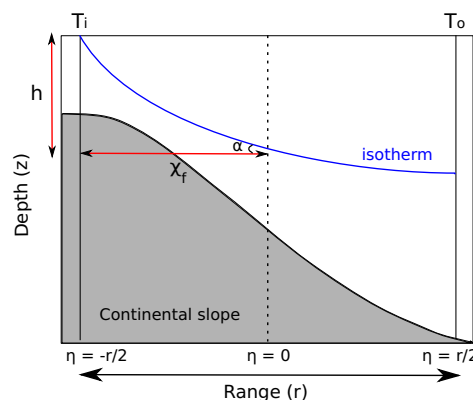


Figure 3: A schematic representation of the coastal upwelling feature model and its parameters.

By using multiscale objective analysis, the theoretical structure of the coastal upwelling was interpolated with the climatological temperature, resulting in a three-dimensional thermal field (Fig. 4). However, this field wasn't an accurate representation of the real thermal field during OAE10 experiment. In order to solve this, we considered that the climatological thermal field correctly describes the vertical variability. Therefore, it is possible to obtain the desired thermal field with a best vertical position of the SACW location (i.e. the one representing the experiment days), by using the vertical

information from climatology in tandem with surface information from remote sensing. This basically means that the subsurface temperature is a function of the sea surface temperature (SST):

$$T(x, y, z) = [T_s(x, y) - T_b(x, y)]\phi(x, y, z) + T_b(x, y), \quad (3)$$

where the subscripts s and b refer to surface and bottoms values, and ϕ are the non-dimensional vertical profiles, which can be obtainable by solving the equation for ϕ using the climatological values. Obtaining ϕ is the process of adimensionalization. This process was applied to build non-dimensional profiles which hold the shape of the typical coastal upwelling temperature profiles, being able to be rescaled according to near-real-time synoptic data.

In the case of this work, the thermal field was redimensionalized using satellite SST data as T_s , and the bottom data from the previous thermal field as T_b . The SST input used for November 18th of 2010 was obtained from the GHRSSST–Group of High Resolution Sea Surface Temperature [23].

Since there were no previous salinity *in situ* data, the final three-dimensional salt field was computed as the meld between climatology and feature model for coastal upwelling, obtained in an analogous form as the temperature (see Eq. 3).

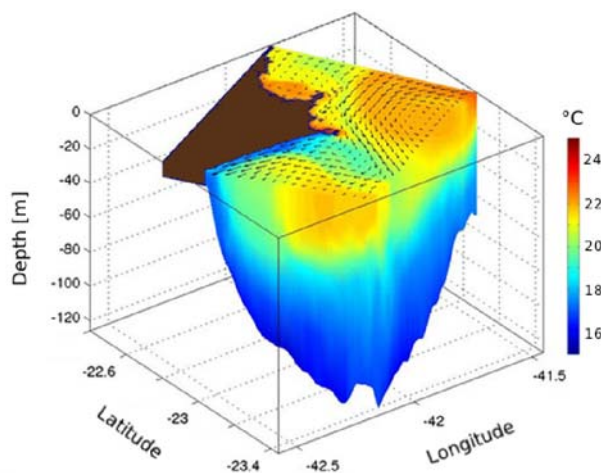


Figure 4: Three-dimensional thermal field after the interpolation between the climatology and the coastal upwelling feature model.

FORMS final product was a 3-D thermohaline field that accurately assimilated the SST conditions for the period of 1 day before the OAE_{x10} experiment (November 18th). This 3-D thermohaline field was employed to initialize a numerical ocean model, in order to forecast the circulation dynamics for the next three days, corresponding to the OAE_{x10} experiment duration (November 19th, 20th and 21th).

2.2.2 The Numerical Ocean Model

ROMS – Regional Ocean Modeling System [24] was the numerical model chosen to provide the ocean forecasts. ROMS is a free-surface, hydrostatic, primitive equation ocean model that uses stretched, terrain-following coordinates in the vertical and orthogonal curvilinear coordinates in the horizontal. This model solves the Reynolds averaged form of the Navier Stokes equations and can be configured in several different ways.

In this work, a grid with horizontal resolution of ≈ 800 m and 25 vertical sigma layers was used. The bathymetry was extracted from digital nautical charts for the region, interpolated to 1 minute of degree resolution. An open boundary condition was applied on the experiment, with the climatology from [25] continuously nudging the domain.

Both wind stress and tides were used to force the model. The wind stress was derived from the level 2 along-track Advanced Scatterometer–ASCAT dataset, and was calculated using the bulk formula [26]. The tidal forcing was obtained from the global model of ocean tides TPXO v7.2 [27].

The numerical model had as initial condition the 3-D mass field resulted from FORMS, and therefore was started for November 18th of 2010, as mentioned above. A prognostic run was performed to predict the fluid state for the future time, and the output of this simulation were used as environmental inputs to an acoustic propagation model, which is described in the next section. Specifically, these environmental inputs were based on a study case for November, 19th, using a 24-hour ocean forecast.

2.3 OCEANOGRAPHIC-MODEL DRIVEN ACOUSTIC PROPAGATION MODELING

The acoustic simulations were performed using the BELLHOP propagation model [28]. BELLHOP is a model for predicting acoustic pressure fields, based on the Gaussian beam tracing method. The feature-oriented ocean forecast provides the necessary range-dependent water column component of the environmental model to initialize BELLHOP. To accomplish this, the predicted field from the oceanographic modeling system output was transformed into sound-speed, using the UNESCO 1983 polynomial [29]. Afterwards, the sound speed was interpolated into the transect containing the acoustic source and hydrophone array, with a suitable grid for acoustic modeling. The acoustic source was located at 10 m depth, emitting 1500-Hz sound signals. The bathymetry used here was the same as for the oceanographic model. The considered boundaries consisted of a free-surface, and an acousto-elastic bottom halfspace.

2.4 ACOUSTIC INVERSION

As mentioned above, this work uses an inversion technique to fine tune the geoacoustic model — namely, through the basement compressional speed — to the acoustic prediction system. The inversion strategy consists on generating several acoustic fields to be compared with acoustic field measures at an hydrophone array. Each computed field is a function of a candidate value of the compressional speed. An exhaustive search on the solution space of the basement compressional speed is carried out, in order to find the value that maximizes $P(\theta)$, an average over frequency of acoustic correlations in space:

$$P(\theta) = \frac{1}{K} \sum_{k=1}^K \mathbf{w}^H(f_k, \theta) \mathbf{R}_{XX}(f_k) \mathbf{w}(f_k, \theta), \quad (4)$$

where $\mathbf{w}(f_k, \theta)$, function of the frequency f_k and the candidate compressional speed θ , is a vector of complex acoustic pressures at the hydrophone array, and $\mathbf{R}_{XX}(f_k, \theta_0)$ is an estimate of the hydrophone correlation matrix at frequency f_k [17].

3 RESULTS AND DISCUSSION

Numerical simulation results are presented in this section, where the forecasted oceanographic field is compared to the field observed on the OAE_{x10} experiment. The aim is to evaluate the performance of the feature-oriented modeling approach for sonar applications. Additionally, the effects of coastal upwelling on the propagation of acoustic energy is assessed here.

After the validation of the ocean forecasts, a new comparison is made between the predicted acoustic field and the OAE_{x10} *in situ* acoustic-data. The correlations obtained in such comparison are described in the present section. At the end, the predicted acoustic field is analyzed before and after the use of acoustic inversion, in order to evaluate the gains achieved by this technique.

3.1 FEATURE-ORIENTED MODELING SKILL FOR ACOUSTIC PREDICTION

As explained in the Sec. 2.2, the initial mass field for ROMS experiments was built upon a regional climatology background melded with the coastal upwelling feature model, consisting in a FORMS initialization scheme. For this reason, the outputs of the ROMS simulations are referred to as feature-oriented ocean forecasts. The current section contains the results of two acoustic simulations with BELLHOP, fed with two different physical fields: (i) the OAE_{x10} ocean-data and (ii) the feature-oriented ocean forecasts. Four 10-km long transects were defined based on the OAE_{x10} ocean-data SST map shown in Fig. 5, in order to observe the influence of different physical patterns on sound propagation characteristics relevant for sonar applications. ROMS outputs were interpolated for the same transects, and sound-speed sections were derived from the ocean-data and the feature-oriented ocean forecasts, respectively (see Fig. 6). Such sections were computed to serve as the initial fields to BELLHOP propagation model. The sections contrast in the range-dependence of bathymetry and sound-speed: section 1 is almost range-independent; sections 2 and 3 are slightly range-dependent; and section 4 is strongly upslope and crosses the upwelling front.

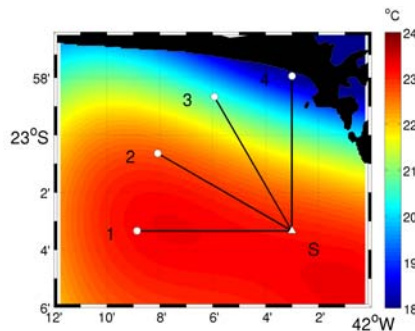


Figure 5: OAE_{x10} ocean-data SST map. The transects 1, 2, 3, and 4 represent the sound-speed sections employed in BELLHOP simulations. The triangle denotes the source position (S), and the circles denote the receivers.

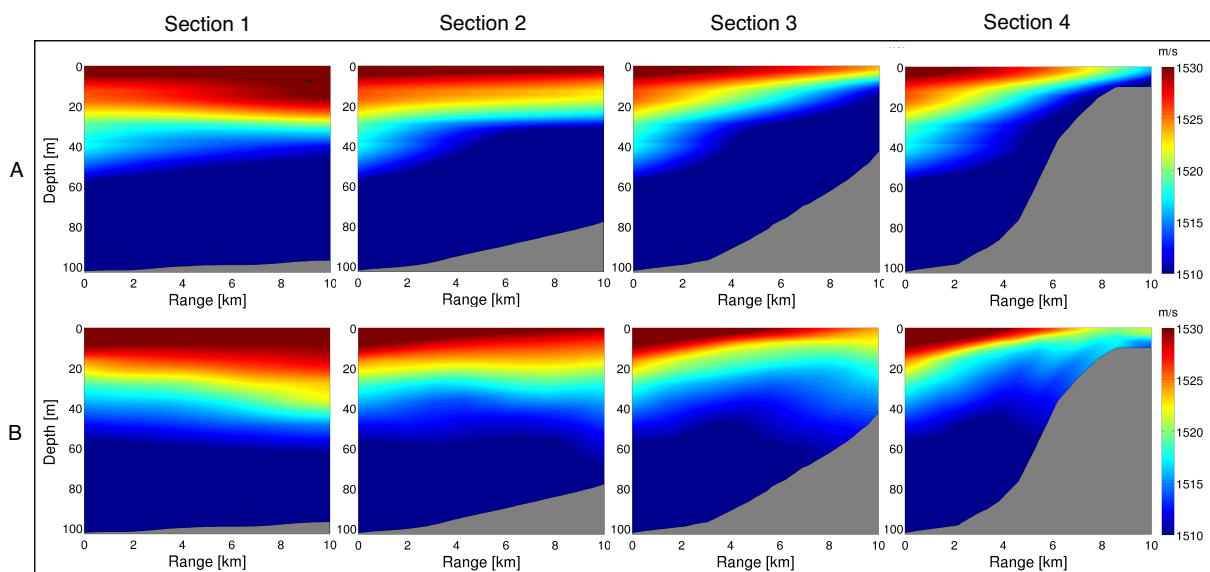


Figure 6: Sound speed sections for the transects in Fig. 5, derived from (A) OAE_{x10} ocean-data, and (B) feature-oriented ocean forecasts.

The difference between the transmission loss (TL) computed with BELLHOP, using the two different sound-speed fields, is plotted in Fig. 7, for each section. The acoustic field is best modeled for the

first 5-km range (area in orange), and the error accumulates with distance. The TL differences exhibit standard deviations ranging between 2.29 and 4.32 dB, acceptable for some sonar applications [2]. In particular, in section 4, no error exists at ranges greater than 7.5 km, due to vanishing acoustic signals predicted with both the *in situ* data and the ocean forecasts. This pattern is the result of the interaction between the acoustic signals and the strong temperature gradient in the upwelling front. Apart from refraction mechanisms, and according to the ray tube concept in ray propagation models, the energy conservation law implies that a decrease in sound speed, along a ray trajectory, will cause the ray tube's amplitude to decrease (assuming no change in the cross-sectional area) [30, p. 164]. As compared to the other sections, the upslope bathymetry is also a determining factor in reducing the range of the acoustic signals, by inducing much higher bottom interaction as water depth decreases, and consequent increase of signal loss [7].

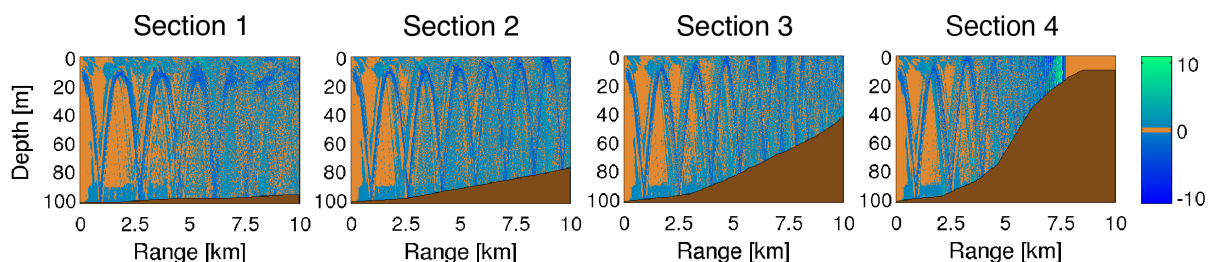


Figure 7: TL errors [dB] for the sections in Fig. 6.

In order to evaluate the relevance of the TL errors for an operational application, the TL predictions are used to calculate the detection probability (DP). To do so, an hypothetical scenario with a passive sonar was considered, using the simulated TL field and typical values for environmental noise and figure of merit (80 dB), to solve the signal excess equation, as proposed in [31]. The BELLHOP-computed acoustic field allowed to calculate the DP, ranging between 0 (no detection capability) and 1 (certain detection). The DP for each section, computed from both the OAE_{x10} ocean-data and the ocean forecasts, is shown in Fig. 8. An interesting result is that, though the subtle differences in the TL fields, the main features of the detection probability were successfully predicted for all sections. It is evident that the simulations using the ocean forecasts had produced a satisfactory spatial distribution of the DP zones, notably matching the simulations initialized by the *in situ* data.

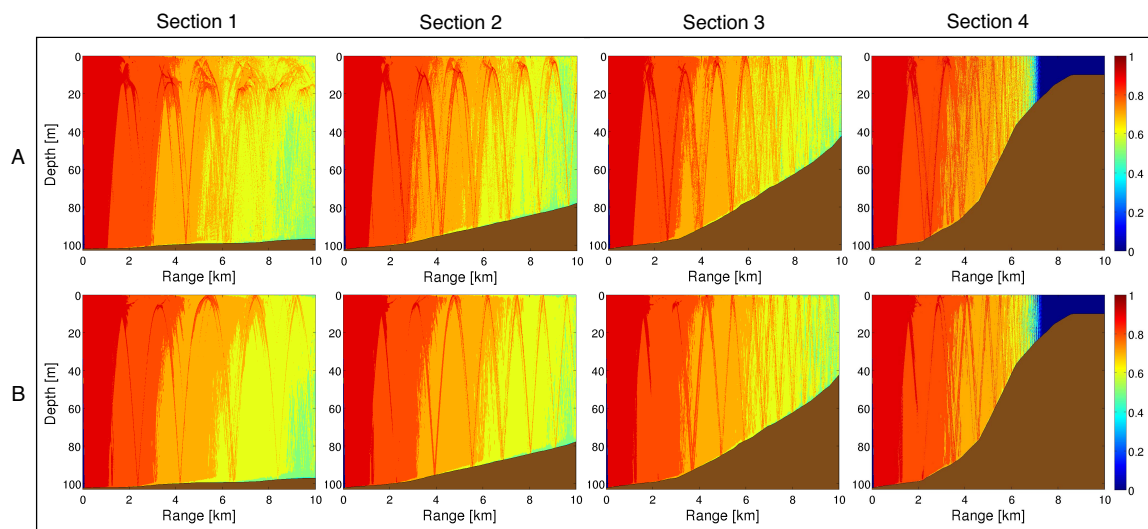


Figure 8: Detection probabilities computed from a passive sonar equation, in which the transmission loss was estimated by BELLHOP, when initialized by (A) OAE_{x10} ocean-data, and (B) feature-oriented ocean forecasts, as corresponding to Fig. 6.

Additionally, it is noted that the coastal upwelling phenomenon imposes severe changes on the detection pattern (Fig. 8 - Section 4). It is clear that the DP becomes close to zero when the acoustic energy crosses the upwelling front (after 7.5-km range), representing the inability for detecting any hypothetical underwater target. This inability is probably a combination of the thermal front effects with the strong upslope bathymetry. The thermal front changes the propagation trajectories, turning the acoustic ray's directions closer to the horizontal, as shown in Fig. 9. This fact implies a decrease of the vertical insonification of the water column. Thus, if the hydrophones are deployed at randomly chosen depths, the probability of receiving the acoustic signal should be lower. This explains how the coastal upwelling acts to reduce the DP, and how important is the synoptic monitoring of such feature for guiding tactical/operational decisions.

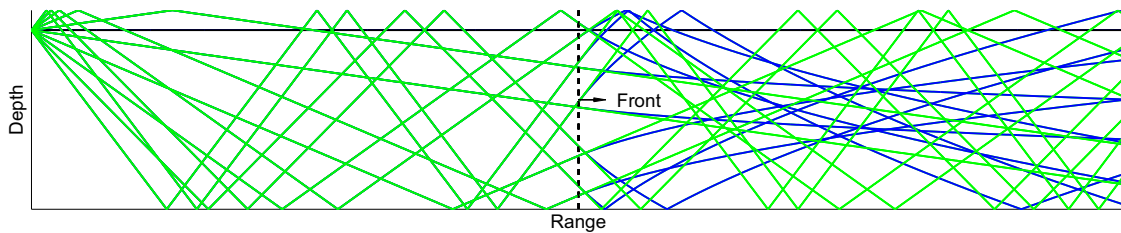


Figure 9: Acoustic ray paths through: i) an homogeneous water column (green line), and ii) an hypothetical upwelling front (blue line).

Considering the correlations between acoustic channel impulse responses (IR), it is revealed that the ocean forecasts lead to acoustic fields whose accuracy degrades with distance, as shown in Fig. 10. This can be explained by an accumulation of propagation errors induced by ocean forecast errors, as the energy travels. Small arrival time errors can imply a large difference in correlation, which is magnified as the distance increases. In zoom, Fig. 11 shows the IR envelopes corresponding to the highest (0.98) and the lowest (0.34) cross-correlation peaks.

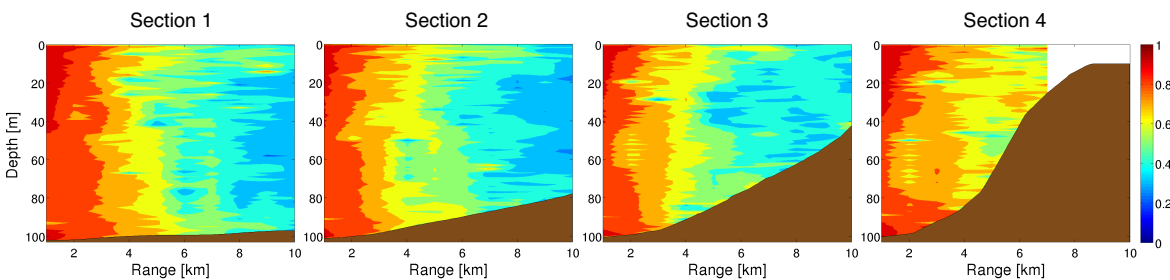


Figure 10: Correlations between IR envelopes modeled with BELLHOP, having as input either the OAE_{x10} ocean-data or the ocean forecasts.

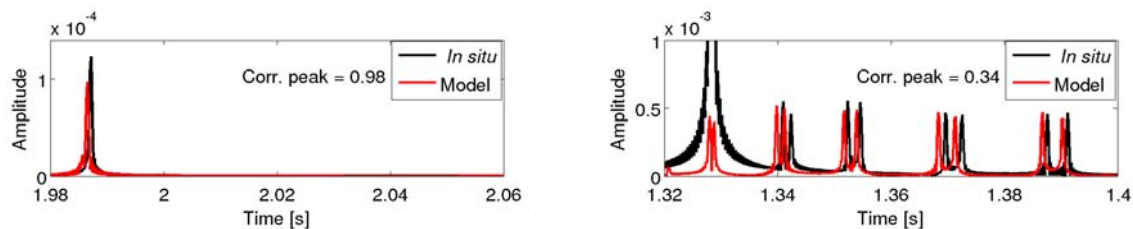


Figure 11: Impulse responses computed from the OAE_{x10} ocean-data (*in situ* – black line), and the ocean forecasts (model – red line), which show the highest and lowest correlation peaks (left and right panels, respectively).

3.2 ACOUSTIC PREDICTION

Having at hand a reliable ocean forecasting system as the one initialized by FORMS, the next step is to gather environmental information regarding geological/geometric properties, and then to use all the above information as environmental input for an acoustic propagation model of choice. As a preliminary study, attention was given only to the geological properties. In this regard, it is common practice to use data from geological archives, nautical charts or historical databases, as input to the acoustic propagation model. Nevertheless, such data can lack accuracy, due to the sparsity of bottom measurements, or to the sometimes merely indicative character of these data [17]. Here, acoustic inversion can play an important role on determining optimal values for the geological (geoacoustic) parameters to be used for modeling acoustic propagation. The complete coupled prediction system proposed in the present work is depicted in Fig. 12. In summary, the components of the environmental model to serve as input for the acoustic propagation model, come from three different sources (Fig. 12 - red box). The water column component is the output of the oceanographic forecast system; the geometric and majority of the geological properties are given by GPS and depth sensors, nautical charts, geological cores, etc.; the basement compressional speed is determined from acoustic inversion, by processing acoustic measures on the oceanic area in which to predict the acoustic field.

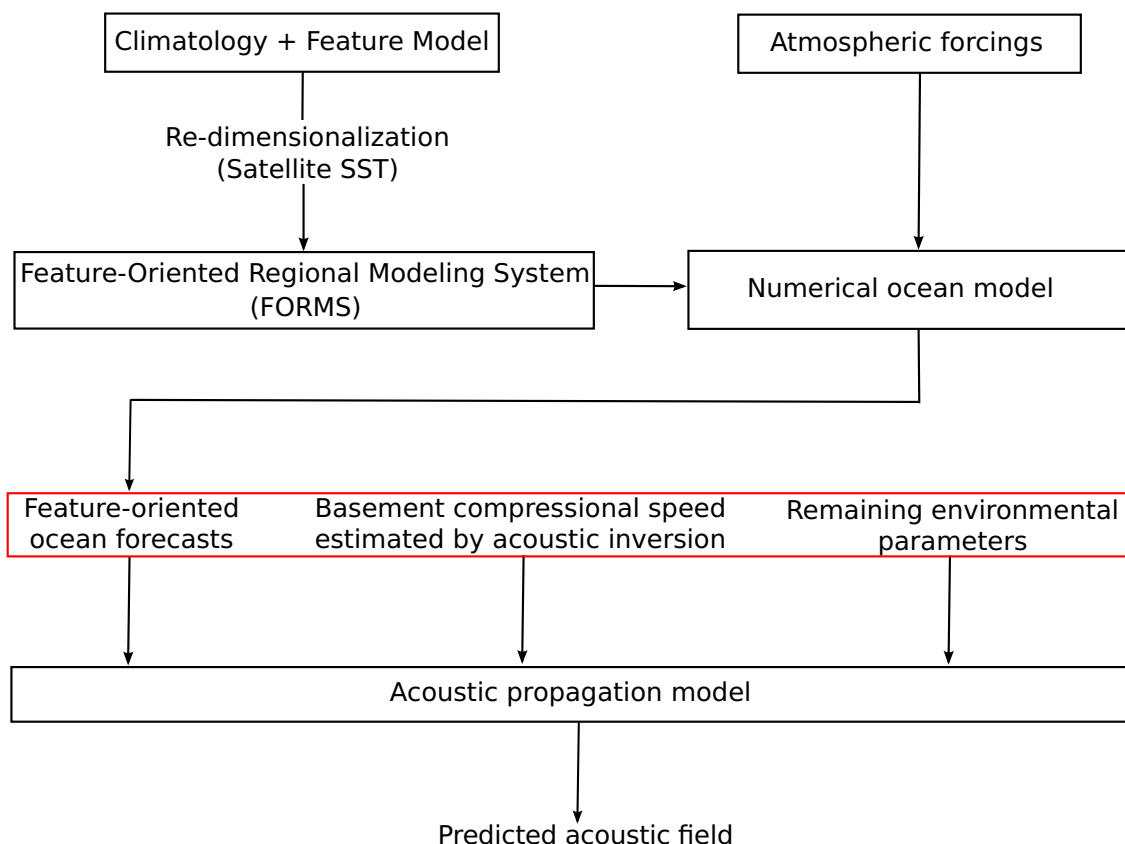


Figure 12: Complete coupled oceanographic-acoustic prediction system.

In order to quantify the effectiveness of acoustic inversion in determining optimal values for the environmental model, two BELLHOP acoustic predictions were carried out using different geoacoustic parametrizations: one from a geological database, and the other from the inversion outcomes. These predictions were compared with acoustic data from the OAE_x10 sea trial, in terms of correlations between IR envelopes. Fig. 13 shows the inversion results in contrast to the baseline values, from geological cores. The difference found between the measured and the estimated properties, apart from noise, is due to inaccuracies in the environmental description provided to BELLHOP, due to the

BELLHOP limitations, and possibly due to real environmental differences between the points of measurement considered for the nautical chart and the transects of acoustic transmission. This difference is the important clue to explain the importance of acoustic inversion: the inversion procedure allowed to estimate the best values of the basement compressional sound speed that guarantee an optimal estimation of the acoustic field at the hydrophone array, using the modeling approach at hand.

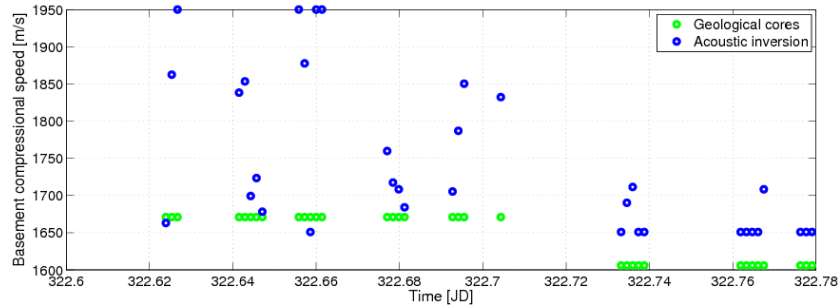


Figure 13: Inversion results for the basement compressional speed (in blue), using 9 tones in the band [500, 2000] Hz. The transmissions covered two different areas, as seen by the two different values given by geological cores (in green).

The compressional speed values obtained from acoustic inversion were used to compute impulse responses for each hydrophone channel, at the same time samples for which the inversion was performed. These impulse responses were correlated with the impulse response estimates computed from the experimental data, with the correlation peaks shown in Fig. 14, right panel. The results show that the basement compressional speed estimates led to increased IR correlation peaks in general (as high as 0.96), as compared to the corresponding values, before the inversion (between 0.72 and 0.86 —see Fig. 14, left panel). It can be seen that the improvements on the acoustic prediction were satisfactory, even when only the compressional speed was inverted for, in other words, tuned for the prediction of the acoustic field.

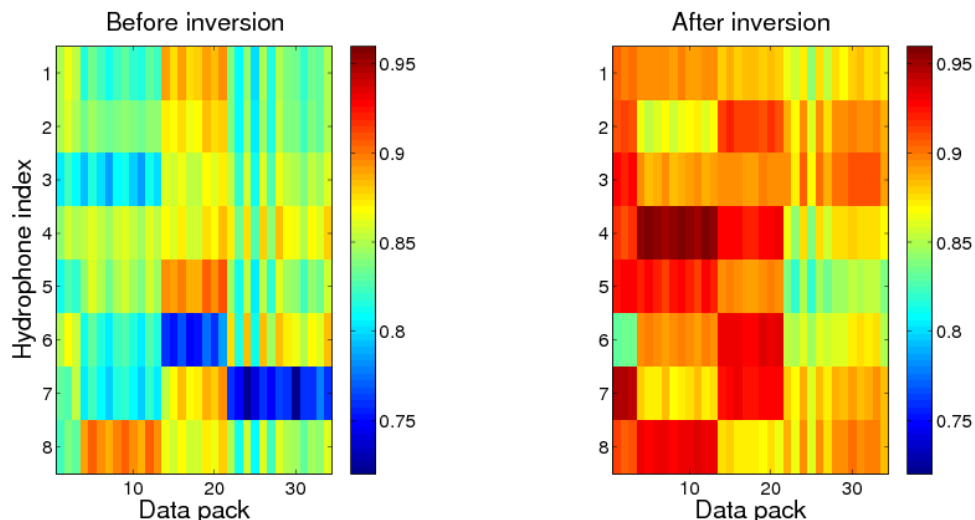


Figure 14: Correlations between predicted and experimental IR envelopes, before (left panel) and after (right panel) the acoustic inversion.

4 CONCLUSIONS

A coupled ocean-acoustic prediction approach was presented for the coastal area of Cabo Frio - Brazil, in the context of the OAE10 sea trial. This approach combines two robust characteristics, re-

garding the oceanography and the acoustics. First, a feature-oriented regional modeling system was used in the initialization of the circulation model at hand. Second, the environmental parametrization of an acoustic propagation model was defined according to both ocean model outcomes and acoustic inversion outcomes.

The feature-oriented ocean forecasts provided a realistic representation of the ocean variability for acoustic purposes. The inclusion of the upwelling feature in the ROMS initial conditions led to an estimated oceanographic field which matches well with the observed *in situ* structure. Simple climatological fields would not include this feature, which would imply a less accurate forecast of the acoustic field, without representing the impact of the upwelling on the strong refraction of acoustic energy. We also found that the inversion technique allowed to calibrate the environmental model parameters of the acoustic propagation model, by acting as a correlator between observed and modeled acoustic fields, whose optimal point gives the parameter values that best model the observed fields. These parameter values allowed to improve the quality of the modeled acoustic impulse responses, as compared to counterparts computed from historical geological data. In summary, the prediction of the acoustic field can be accomplished by combining a feature-oriented ocean modeling approach with an acoustic inversion scheme, with important scientific/operational consequences.

In the present feasibility study, the environmental outcomes from acoustic inversion were used to make synchronous acoustic predictions. Future work will use the acoustic inversion outcomes at present times, to predict the acoustic field at future times. Moreover, further work should be devoted to the use the acoustic inversion outcomes to be inserted into the ocean dynamic modeling system, in a way to minimize the overall acoustic errors.

ACKNOWLEDGMENTS

This work was developed within the framework of the research project 'Ocean Acoustic Exploration (OAE)', funded by the European Union (contract OAE - 230855), and the research project 'DetectFeicoes', funded by the FAPERJ (contract E-26/110.327/2012). Thanks are due to the Brazilian Navy, for providing the human/material resources for the sea trial, and supporting this research.

REFERENCES

1. W. Kuperman and J. Lynch. Shallow-water acoustics. *Physics Today*, 57: pp. 55–61, 2004.
2. A. R. Robinson, P. Abbot, P. Lermusiaux, and L. Dillman. Transfer of uncertainties through physical-acoustical-sonar end-to-end systems: a conceptual basis. In *Acoustic Variability*, pp. 603–610. Kluwer Academic Press, N.G. Pace and F.B. Jensen edition, 2002.
3. P. Abbot and I. Dyer. Sonar performance predictions based on environmental variability. In *Acoustic Variability*, pp. 611–618. Kluwer Academic Press, 2002.
4. A. Robinson and P. Lermusiaux. Prediction systems with data assimilation for coupled ocean science and ocean acoustics. In *Proc. of the Sixth International Conference on Theoretical and Computational Acoustics*. World Scientific Publishing Co., 2004.
5. F. Lam, P. Haley, J. Janmaat, P. Lermusiaux, W. Leslie, M. W. Schouten, L. Raa, and M. Rixen. At-sea real-time coupled four-dimensional oceanographic and acoustic forecasts during Battlespace Preparation 2007. *Journal of Marine System*, : pp. 306–320, 2009.
6. P. Lermusiaux, C.-S. Chiu, and A. Robinson. Modeling uncertainties in the prediction of the acoustic wavefield in a shelfbreak environment. In *Theoretical and Computational Acoustics*, pp. 191–200. World Scientific Publishing Co., 2002.
7. P. Lermusiaux, J. Xu, S. Chen, S. Jan, L. Chiu, and Y. Yang. Coupled ocean-acoustic prediction of transmission loss in a continental shelfbreak region: predictive skill, uncertainty quantification and dynamical sensitivities. *Journal of Oceanic Engineering*, 35(4), October 2010.

8. A. Gangopadhyay and A. Robinson. Feature-oriented regional modeling of oceanic fronts. *Dyn. Atmos. Oceans*, 36(1-3): pp. 201–232, 2002.
9. L. Calado, A. Gangopadhyay, and I. C. A. Silveira. Feature-oriented regional modeling and simulations (FORMS) for the western South Atlantic: Southeastern Brazil region. *Ocean Modell.*, 25(1-2): pp. 48–64, 2008.
10. J. Cummings, C. Szczechowski, and M. Carnes. Global and regional ocean thermal analysis systems. *Mar. Technol. Soc J.*, 31(6375), 1997.
11. L. Calado, I. C. A. Silveira, A. Gangopadhyay, and B. M. Castro. Eddy-induced upwelling off Cape São Tomé (22°S, Brazil). *Cont. Shelf Res.*, 30: pp. 1181–1188, 2010.
12. A. Gangopadhyay, P. Lermusiaux, L. Rosenfeld, A. Robinson, L. Calado, H. Kim, W. Leslie, and P. H. Jr. The California Current System: a multiscale overview and the development of a feature-oriented regional modeling system (FORMS). *J. Atmos. Ocean. Tech.*, 14(6), 2011.
13. A. Robinson and D. Lee. *Oceanography and Acoustics - Prediction and Propagation Models*. American Institute of Physics, 1 edition, May 1997.
14. J. Small, L. Shackelford, and G. Pavey. Ocean feature models - their use and effectiveness in ocean acoustic forecasting. *Annales Geophysicae*, 15: pp. 101–112, 1997.
15. O. Carrière, J.-P. Hermand, L. Calado, A. De Paula, and I. C. A. Silveira. Feature-oriented acoustic tomography: Upwelling at Cabo frio (Brazil). No. 09. *IEEE J. Ocean. Eng.*, October 2009.
16. G. Codato, W. Watanabe, L. Calado, N. Martins, and A. Ramos. A influência da frente térmica da ressurgência costeira de Cabo Frio na perda do sinal acústico. *A Ressurgência*, 06, 2012.
17. N. Martins, C. Soares, and S. Jesus. Environmental and acoustic assessment: The AOB concept. *Journal of Marine Systems*, 69: pp. 114–125, 2008.
18. N. Martins and S. Jesus. Bayesian acoustic prediction assimilating oceanographic and acoustically inverted data. *Journal of Marine Systems*, 78: pp. S349–S358, 2009.
19. L. Calado, A. Gangopadhyay, and I. C. A. Silveira. A parametric model for the Brazil Current meanders and eddies off Southeastern Brasil. *Geophys. Res. Lett.*, 33: p. L12602, 2006.
20. L. Miranda. Forma de correlação T-S de massas de água das regiões costeiras e oceânicas entre o Cabo de São Tomé - RJ e a ilha de São Sebastião - SP, Brasil. *Bolm. Inst. Oceanogr.*, 33(2): pp. 105–119, 1985.
21. R. A. Locarnini, A. Mishonov, J. Antonov, T. Boyer, H. Garcia, and S. Levitus. World Ocean Atlas 2005. *NOAA Atlas NESDIS*, 1(61): p. 182, 2006.
22. C. Shaji and A. Gangopadhyay. Synoptic modeling of the west India Coastal Current System using an upwelling feature model. *Cont. Shelf Res.*, 24: pp. 877–893, 2007.
23. T. G. S. Team. *Users Manual for the Group for High Resolution Sea Surface Temperature (GHRSSST-PP) Draft V1.2*, GHRSSST/17 edition, July 2008.
24. A. Shchepetkin and J. McWilliams. The regional ocean modeling system (ROMS): a split-explicit, free-surface, topography following coordinates ocean model. *Ocean Modell.*, 9(4): pp. 347–404, 2005.
25. T. Boyer, S. Levitus, H. Garcia, R. A. Locarnini, C. Stephens, and J. Antonov. Objective analyses of annual, seasonal, and monthly temperature and salinity for the world ocean on a 0.25 degrees grid. *Int. J. Climatol.*, 25(7): pp. 931–945, Jun 2005.
26. W. Large and S. Yeager. *Diurnal to decadal global forcing for ocean and sea-ice models: The data sets and flux climatologies*. Tech. Report 460, 2004.

27. G. Egbert and S. Erofeeva. Efficient inverse modeling of barotropic ocean tides. *Journal of Atmospheric and Oceanic Technology*, 19: pp. 184–203, Feb 2002.
28. M. Porter and H. Bucker. Gaussian beam tracing for computing ocean acoustic fields. *J.A.S.A.*, 82(4): pp. 1348–1359, 1987.
29. P. Fofonoff and R. C. J. Millard. *Algorithms for computation of fundamental properties of seawater*. UNESCO Tech. Pap. in Mar. Sci., 1983.
30. F. Jensen. *Computational Ocean Acoustics*. Modern Acoustics and Signal Processing. Springer Science+Business Media, LLC, 2011.
31. C. Ferla and M. Porter. Receiver depth selection for passive sonar systems. *IEEE J. Ocean. Eng.*, 16(3): pp. 267–279, July 1991.